Near Surface Strain Measurements On Quartz Wafers and Devices

A key factor in understanding the behaviour of silicon and quartz devices, such as microelectronic components and piezoelectric transducers, is the ability to accurately map the strain distributions in these devices. This information would assist in optimising fabrication processes and determining performance limits as a function of axial forces, bending moment, torque, pressure, acceleration and temperature. Optical techniques, such as photo-elasticity, are limited by the spatial resolution, which is insufficient to provide detailed information on devices as small as 5-6 mm wide and 10 mm long. Hence, a study was carried out to investigate alternative methods for determining the strain distribution in quartz wafers and quartz devices.

This Measurement Note considers the use of X-ray diffraction (XRD), Raman spectroscopy and electronic speckle pattern interferometry (ESPI) for measuring the near surface strain distribution in quartz devices under various loading conditions. The three techniques are assessed in terms of information provided, spatial resolution (or sensitivity), specimen preparation requirements, equipment cost, inspection speed, complexity of data analysis and the practicality of using the technique for field measurements. The research included in-situ inspection of surface acoustic wave (SAW) devices subjected to torque loading.

This Measurement Note was prepared as a result of investigations undertaken within the DTI funded programme "Measurements for Materials Systems (MMS)" in collaboration with Sensor Technology Ltd, Transense Technologies Plc and Crane Electronics Ltd. The work involved NPL Materials Centre and Centre for Optical and Analytical Measurement.

W R Broughton, A T Fry, D -A Mendels and C J Chunnilall

July 2003

INTRODUCTION

Optical techniques, such as photo-elasticity, have insufficient resolution to enable strain mapping of quartz devices (typically 5 mm x 10 mm), and thus alternative techniques need to be considered. This Measurement Note considers the use of X-ray diffraction (XRD), Raman spectroscopy and electronic speckle pattern interferometry (ESPI) for measuring the near surface strain distribution in quartz devices under various loading conditions. These techniques are assessed in terms of information provided, spatial resolution (or sensitivity), specimen preparation requirements, equipment cost, inspection speed, complexity of data analysis and the practicality of using the technique for in-situ and field measurements.

X-RAY DIFFRACTION (XRD)

XRD was used to measure strain levels in quartz wafers and surface acoustic wave (SAW) devices at various stages of production and under torque loading.

Residual Strain Measurements

Residual strain measurements were performed using a Siemens D500 diffractometer and Cr-Ka radiation (see Figures 1 and 2). This comprised of a D500 goniometer that was set up in the Bragg-Brentano geometry with a θ-2θ drive. The X-ray generator was a Kristalloflex model with a solid-state scintillation detector attached to the 2θ-drive. A full 2θ scan was conducted of the samples in order to determine a suitable peak (q_0 = 40.078464°) for the measurement of residual strain.

Residual strains were measured in the "as-received" state, where one side had been mechanically polished and the other side had been ground. Residual strain measurements were performed at nine locations on the surface (Figure 3). For these measurements, the residual strain was determined using the **d** versus $\mathbf{sin^2}y$ (y = angle of inclination between sample and incident beam) technique using omega geometry to evaluate the magnitude of the residual strain.

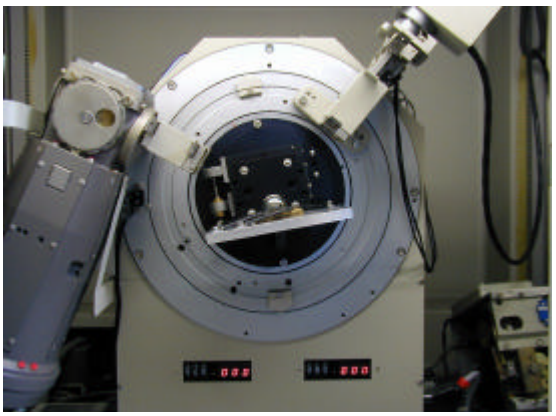

Figure 1: Siemens D500 Diffractometer.

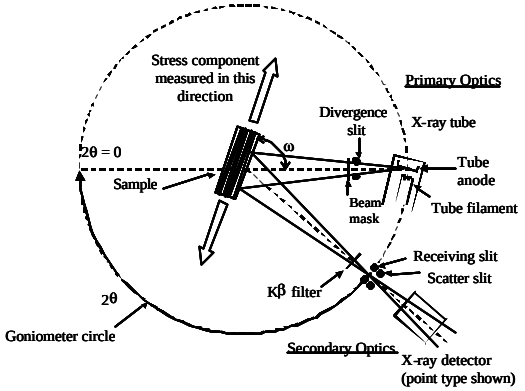

Figure 2: Schematic of XRD system.

The residual strain measurements on the ground surfaces of the "as-received" quartz wafers are highly compressive, ranging from -0.6 to -1.6 % (see Table 1 and Figure 4) with maximum strain levels located at the wafer centre and decreasing towards the wafer edges. Counterbalancing tensile strains of equivalent magnitude can be expected to be present on the polished surface of the wafers.

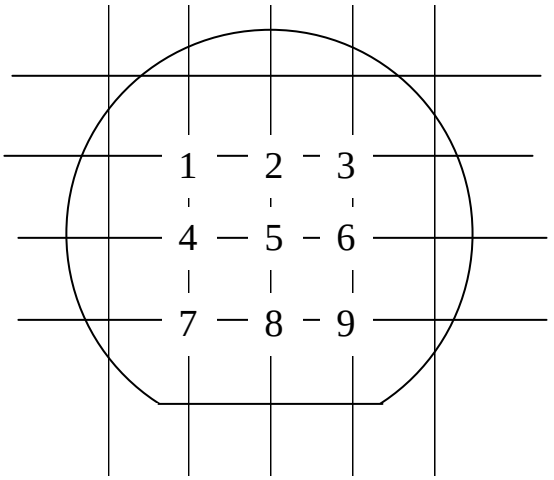

Figure 3: XRD measurement sites.

Table 1: Measured Residual Strain in "As-Received" Quartz Wafers

Position	Residual Strain (%)				
	AAAB	AAAC	AAAD	AAAE	AAAF
1	-1.013	-1.440	-1.453	-1.125	-1.602
2	-1.176	-1.218	-1.140	-1.493	-1.431
3	-1.125	-1.471	-1.168	-1.416	-1.410
4	-1.198	-1.619	-1.453	-1.477	-1.443
5	-1.043	-1.431	-1.525	-1.416	-1.172
6	-1.126	-1.172	-1.451	-1.475	-1.423
7	-0.610	-1.399	-1.421	-1.393	-1.346
8	-0.692	-1.316	-1.494	-1.427	-1.214
9	-0.787	-1.258	-1.262	-1.150	-1.294

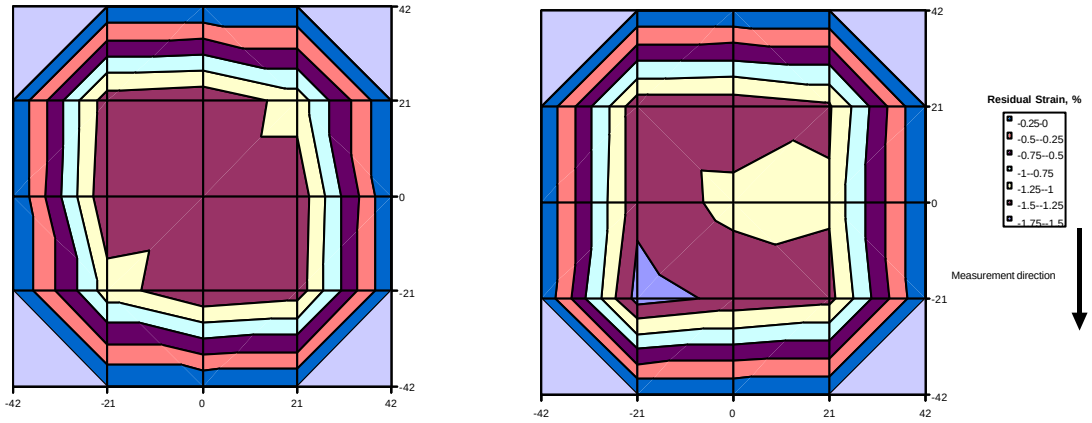

Figure 4: Residual strain maps for "as-received" quartz wafers AAAE and AAAF.

The strain distribution pattern for most of the wafers was similar; as expected if produced by the same procedure. The XRD detector used was relatively slow, thus it was not feasible from a time perspective to increase the resolution. Sampling speed is dependent on the type of detector used, and a recent update of the system now samples within 10 seconds. The information obtained using only nine locations provided sufficient information on the strain distribution in the wafers. The technique can be used to provide a through-thickness strain profile, however the process used would be destructive.

In-Situ Strain Measurements

Strain measurements were carried out on one of two SAW devices (see Figure 5), which were mounted on a rectangular beam (5 mm x 12.5 mm) to measure the direct (tensile and compressive) strain components of the shear strain.

The gauge-length of the beam was nominally 100 mm. The end sections of the beam were circular to fit the torque loading rig (see Figure 6) with a diameter of 12.5 mm. The SAW devices were adhesively bonded to the flat surfaces using M-Bond 610 epoxy adhesive at orientation of ±45° to the longitudinal axis of the beam.

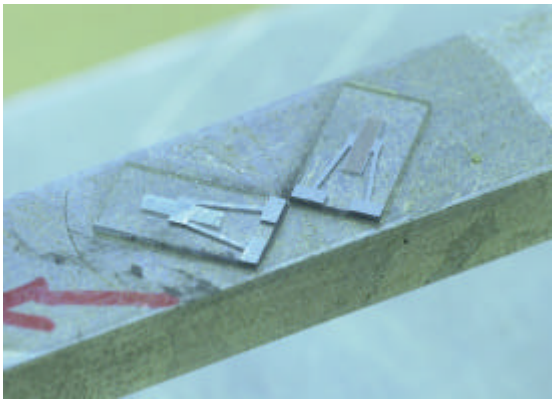

Figure 5: Surface acoustic wave (SAW) devices mounted on torque beam.

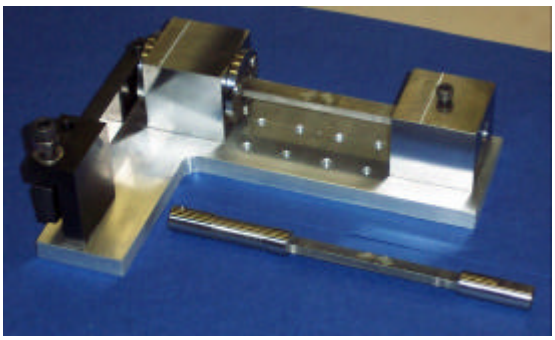

Figure 6: Torque loading rig and specimen.

Torque was applied to the beam via a loading rig (Figure 6) and the corresponding strains on the surface of the SAW device (see Figure 5) were measured using XRD by comparing the stressed and unstressed lattice spacing **d** and $\mathbf{d_0}$ positions using the following relationship:

$$e_{fy}^{\{hkl\}} = \ln\left(\frac{d_{fy}}{d_0}\right) = \ln\left(\frac{\sin q_0}{\sin q_{fy}}\right)$$

where the value of $\mathbf{d_0}$ is obtained from published literature and **d** is measured. q denotes the angle of the diffraction peak.

The incident beam was focused along the axis of the SAW devices and not along the beam (i.e. specimen) axis. Shifts in the diffraction peak caused by twisting of the beam were corrected using a standard silicon powder. An applied displacement of 3.6 mm (via the loading arm) is equivalent to an applied torque of 13 Nm (or 1,000 με at the centre of the beam). Strain measurements using the 40.014° peak are presented in Table 2 and Figure 7.

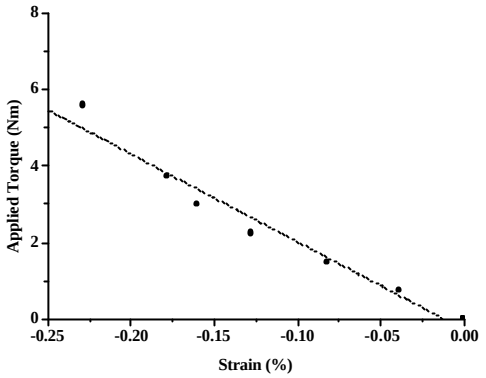

Figure 7: XRD strain measurement versus applied torque.

The relationship between applied torque and resultant strain as measured using XRD can be considered linear in the torque range of 0 to 4 Nm. The applied torque versus XRD strain curve starts to deviate from linearity beyond this range. It should be noted that the XRD beam interrogates a region roughly 10 mm long and 1-2 mm wide, hence strain measurements are associated with a rectangular strip on the surface of the torque transducer rather than an average strain value over the entire area sampled by the transducer. In addition, the distribution of shear stress in the beam section is not uniform along the beam or through the beam within the gauge-length.

XRD is a research tool and not easily adaptable for in-service monitoring of strain distributions, particularly under dynamic conditions. However, portable commercial equipment is available. Although analysis is complex, the technique can be used to map the average strain as a function of applied load.

Table 2: Applied Torque Versus Longitudinal Strain in SAW Device

Deflection (mm)	Applied Torque (Nm)	Applied Strain on Beam	Peak position, ?	Strain, e_{fy} (%)
0	0.0000	0.00	40.078464	0.0000
0.2	0.7448	55.41	40.094124	-0.0391
0.4	1.4896	110.83	40.111302	-0.0819
0.6	2.2344	166.24	40.129809	-0.1280
0.8	2.9792	221.66	40.142594	-0.1599
1.0	3.724	277.07	40.149823	-0.1779
1.5	5.586	415.61	40.170394	-0.2291

RAMAN SPECTROSCOPY

An alternative approach is to use Raman spectroscopy rather than XRD to determine the strain distribution near the surface of quartz devices. The use of the technique for determining strain relies on detecting frequency shifts in Raman modes (phonons) under mechanical stress. The magnitude of the shift is proportional to the strain. Figure 8 shows a schematic diagram depicting inelastic (Raman) scattering from α–quartz (SiO_2) in which the frequency and intensity (peak height) of the scattered peak changes with stress. By monitoring the Raman scattering frequency at different positions on the sample, a strain map can be produced with a spatial resolution of 0.01 mm. Raman spectroscopy systems are capable of measuring frequency changes as small as 0.02 cm^{-1}. For silicon, this corresponds to a stress sensitivity of 10 MPa.

The Raman scattering frequency of silicon is 521 cm^{-1}. However, this frequency is dependent on the strain state of the material (i.e. residual strains will cause the peak to shift). In general, compressive stresses result in an increase in Raman frequency and conversely tensile stresses cause a reduction. The relation between strain or stress and the Raman frequency tends to be linear under uniaxial and biaxial loads.

A Dilor XY spectrometer was used, together with an Ar^+ laser, and a liquid nitrogen cooled CCD detector, to obtain spectra from the quartz wafer used as a torque sensor. In the Dilor instrument, incident laser light from an Ar^+ laser is focused on a sample (Figure 8). The scattered light is analysed using a double grating monochromator followed by a single grating spectrometer. A cooled CCD detector allows weak signals to be measured. A microscope objective lens combined with confocal optics, allows the signal to be collected from sample volumes on the micrometer scale. A stepper-driven XY translation stage enables high spatial resolution spectral mapping.

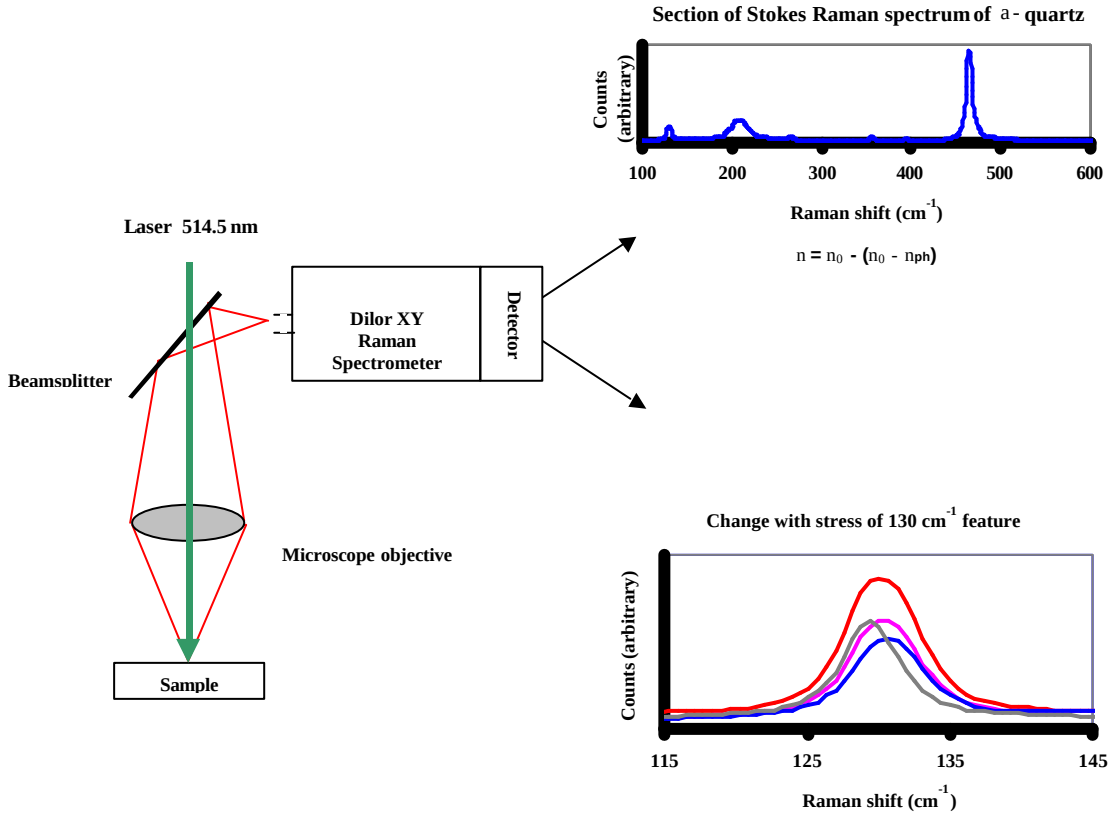

Figure 8: Schematic of scattering from a -quartz (SiO_2). (Dilor XY Raman spectrometer)

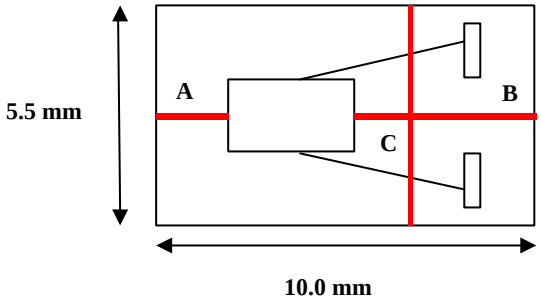

Figure 9: Mapping positions on SAW transducer for Raman spectroscopy.

Strain measurements were carried out on the torque device shown in Figures 5 and 6. Measurements were taken at 11 equally spaced intervals along three lines **A** (2.00 mm long), **B** (3.40 mm long) and **C** (5.50 mm long) on the SAW device (see Figure 9). The Raman frequency measurement range was 70 cm^{-1} to 675 cm^{-1} (Figure 10) Strain measurements were obtained for four different levels of applied torque (0.0, 1.8, 3.6 and 5.4 Nm). A x50 microscope objective was used to irradiate the sample with ~40 mW of 514.5 nm laser radiation, and also used to collect the back-scattered light. The measurement time at each position was approximately 3 minutes.

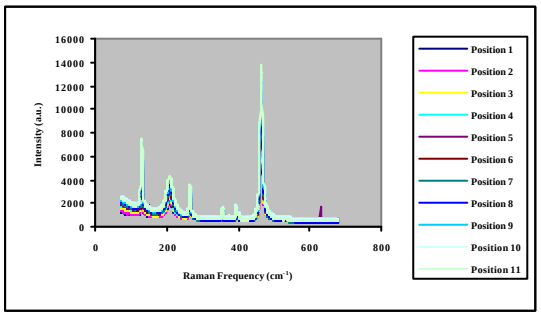

Figure 10: Raman spectrum along line B as a function of position: Position 1 = edge and Position 11 = centre.

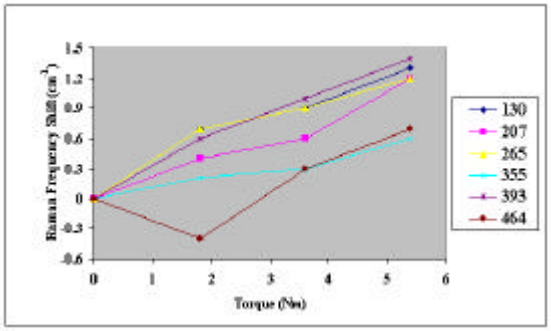

Figure 11: Raman frequency shift as a function of applied torque.

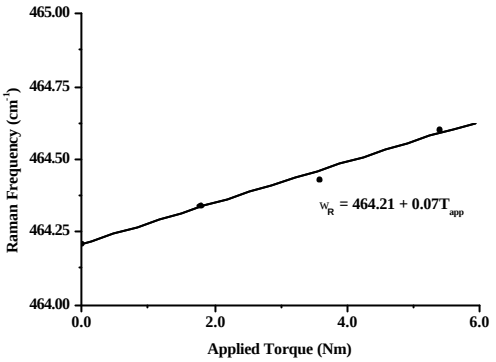

Figure 12: Raman frequency shift (464 cm^{-1}) at Position 6 on line C.

α-quartz (SiO_2) has a rich Raman spectrum with 14 bands spanning the range 100 cm^{-1} to 1300 cm^{-1}. An initial trial was carried out at a single point on the surface of one of the torque loaded SAW devices to determine the relationship between the Raman frequency shift and applied torque. Several different Raman features (130, 207, 265, 355, 393 and 464 cm^{-1}) were monitored. The 464 cm^{-1} Raman peak is generally selected for determining strain in quartz. The Raman frequency shift was positive (increase in frequency) and tends to increase linearly with applied torque (see Figures 11 and 12). The results shown in Figure 12 were from a separate location.

The technique is able to provide information on the strain response within the quartz substrate to applied load. The Raman frequency shift, which is independent of focal path is normally used for measuring localised strain. Whereas, the peak height is dependent on both the strain state of the inspected area and the separation distance between the optical microscope objective lens and the inspected surface. In order to use the peak height, the beam needs to be focused identically at each location on the sample surface; a difficult task on structures that have undergone out-of-plane deformation as a result of twisting. Another issue relates to the complexity of resolving strain components under a biaxial stress state. The technique is readily adaptable to uniaxial loading conditions, but would require additional experimental and analysis work in order to interpret the data in terms of strain measurement.

ELECTRONIC SECKLE PATTERN INTERFEROMETRY (ESPI)

ESPI was used to monitor the out-of-plane displacement of the torsion bar shown in Figure 5. The specimen preparation was relatively straightforward (only requiring the spraying of a chalk spray on the surface of the specimen). ESPI is a non-contact measurement, based on the interference between two diffracted light patterns, which require a certain roughness of the surface [1-2]. A layout of the ESPI system is shown in Figure 13. Experiments were carried-out on an optical table in an enclosed environment, thereby minimising vibration from the environment.

A maximum displacement of approximately 100 μm per step can be applied to the lever of the torsion jig, by means of a piezoelectric linear step motor, with a resolution of approximately 4 nm. It was found, however, that a displacement of 10-20 μm was sufficient to obtain 3 fringes (each fringe corresponds to 0.415 μm z-displacement). Figure 14 shows a typical speckle pattern resulting from out-of-plane deformation of a surface of a rectangular rod loaded in tension. The plot shown in Figure 15 is typical of the strain state present at the surface of a rectangular rod under torsion. It is possible to convert the data presented in these plots into actual strain values using classical beam analysis, and deduce the average strains of the surface in three orthogonal directions. However, it was not possible to distinguish the specific strain in the sensor from the strain on the rod, although in some specific cases a pattern resembling a "Y" shape could be observed.

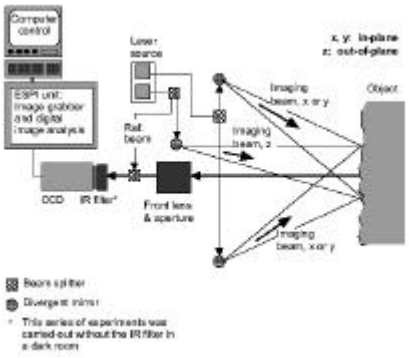

Figure 13: ESPI system layout [2].

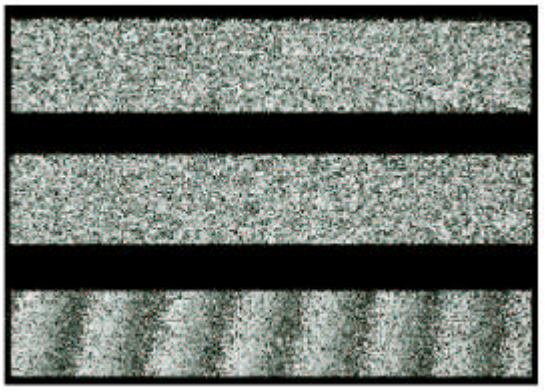

Figure 14: A typical speckle pattern resulting from out-of-plane deformation: undeformed (top); deformed (middle); and difference (bottom) [2].

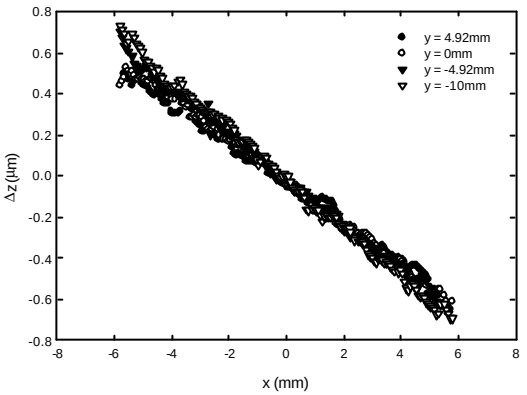

Figure 15: Out-of-plane deformation measurements on torque bar using ESPI.

In order to obtain reliable strain measurements at the surface of quartz devices using ESPI, the rigidity (**EI** where **E** is the elastic modulus and **I** is the moment of inertia) of the rod and the attached device should be of similar magnitude.

Although the sensitivity of the ESPI apparatus is high, with a minimum displacement in the range of 20 nm detectable, it was not possible to optically resolve strain variations across the SAW device. Some slight variations were detected at the edges of the SAW device, but could not be analysed, due to a lack of sensitivity of the detection equipment.

CONCLUSIONS

XRD proved a useful tool for identifying changes in strain state as a result of the various processing stages and changes in applied load. Further work is required to establish a relationship between the XRD measurements and engineering strain measurements. This would require the use of an accurate calibration specimen subjected to known loading conditions with the engineering strains measured independently using either contact or non-contact techniques or the SAW device properties (i.e. frequency response). The use of an accurate calibration specimen also applies to Raman spectroscopy. The technique would need further investigation in order to establish a relationship between Raman frequency shift and engineering strain measurements. ESPI proved ineffective in distinguishing between the strains in the sensor and strains present at the surface on the rod, although in some specific cases a pattern resembling the shape of the metallic "Y" could be observed. The inability to detect strain variations at the surface of the SAW device was due to rigidity of the rod (EI), which was too large in comparison with the rigidity of the device. The technique in principle should enable rapid and accurate strain mapping across and along the beam, and also allow for resolving the strain components.

REFERENCES

1. *The Use of Electronic Speckle Pattern Interferometry for Determining Non-Uniform Strain Fields*, J. Niklewicz and G.D. Sims, NPL Measurement Note, CMMT(MN)056, 1999.
2. *Detection of Sub-Surface Defects in Multi-Layered Polymer Composites*, D.-A. Mendels and R. Shaw, NPL Measurement Note MATC(MN)17, 2002.

ACKNOWLEDGEMENTS

The work was undertaken with the support of the United Kingdom Department of Trade and Industry in collaboration with Sensor Technology Ltd, Transense Technologies Plc and Crane Electronics Ltd and forms part of the Measurements for Materials Systems (MMS) Studio Project "Quality of Bonded Surface Acoustic Wave Devices". The authors would like to express their gratitude to their colleagues at the National Physical Laboratory, particularly Miss Elena Arranz, Mr Bruce Duncan, Mr Nicolas Evanno, Mr Dipak Gohil and Mr Richard Shaw.

For further information contact:

Dr Bill Broughton
NPL Materials Centre
National Physical Laboratory
Queens Road, Teddington
Middlesex, TW11 0LW
Telephone: 020-8977 3222 (*switchboard*)
Direct Line: 020-8943 6834
Facsimile: 020-8943 6177